Banding and Polarity of Actin Filaments in Interphase and Cleaving Cells

JEAN M. SANGER and JOSEPH W. SANGER
Department of Anatomy, School of Medicine, University of Pennsylvania, Philadelphia, Pennsylvania 19104

ABSTRACT Heavy meromyosin (HMM) decoration of actin filaments was used to detect the polarity of microfilaments in interphase and cleaving rat kangaroo (PtK_2) cells. Ethanol at −20°C was used to make the cells permeable to HMM followed by tannic acid-glutaraldehyde fixation for electron microscopy. Uniform polarity of actin filaments was observed at cell junctions and central attachment plaques with the HMM arrowheads always pointing away from the junction or plaque. Stress fibers were banded in appearance with their component microfilaments exhibiting both parallel and antiparallel orientation with respect to one another. Identical banding of microfilament bundles was also seen in cleavage furrows with the same variation in filament polarity as found in stress fibers. Similarly banded fibers were not seen outside the cleavage furrow in mitotic cells. By the time that a mid-body was present, the actin filaments in the cleavage furrow were no longer in banded fibers. The alternating dark and light bands of both the stress fibers and cleavage furrow fibers are approximately equal in length, each measuring ~0.16 μm. Actin filaments were present in both bands, and individual decorated filaments could sometimes be traced through four band lengths. Undecorated filaments, 10 nm in diameter, could often be seen within the light bands. A model is proposed to explain the arrangement of filaments in stress fibers and cleavage furrows based on the striations observed with tannic acid and the polarity of the actin filaments.

The most prominent constituent of both stress fibers and cleavage furrows is actin in the form of microfilaments (17, 21, 32–36). Myosin and α-actinin, also, have been identified with immunofluorescent labeling techniques in both of these systems (11, 12, 15, 23, 51), and tropomyosin has been found in stress fibers (22). The function of the cleavage ring is obviously contractile, and the stress fibers, although often referred to as cytoskeletal elements, may develop contractile forces as well (4, 19, 40).

Because the proteins found in stress fibers and contractile rings have their counterparts in muscle cells, the obvious question is: how similar is the manner of force production in the nonmuscle systems to the sliding filament mechanism found in striated muscle cells. In muscle, actin microfilaments are anchored at one end to Z disks (cross-striated muscles) or dense bodies (molluscan smooth muscles) so that all the filaments, extending in one direction from a Z disk (18) or dense body (49) have the same polarity. This polarity can be visualized by addition of heavy meromyosin (HMM) which projects in arrowhead configuration from the actin filaments resulting in arrowheads which always point away from the Z band or dense body to which the filaments are attached (18, 49). Each muscle sarcomere consists of two sets of oppositely polarized actin filaments attached to Z bands, plus centrally positioned bipolar myosin filaments which interact with the interdigitating actin filaments (17, 18).

The highly ordered and stable contractile apparatus of cross-striated muscle cells is obviously not present in nonmuscle cells, although many of the contractile proteins are. Of the two interacting myofilaments, actin and myosin, only actin filaments can be demonstrated unambiguously on an ultrastructural level in nonmuscle cells. Recently, oppositely polarized actin filaments have been observed in stress fibers by Begg et al. (3), suggesting a possible sliding mechanism. We have used a new way to make cells permeable to HMM which involves plunging the cells into cold (−20°C) ethanol for 5 min. This method when coupled with the tannic acid-glutaraldehyde fixation procedure of Begg et al. (3), results in preservation of cells which is superior to that obtained when glycerol is used to make the cells permeable. Striations seen in some stress fibers ultrastructurally (13, 14, 33) and with immunofluorescence (22, 24, 51, 54) were also seen in these ethanol-treated

THE JOURNAL OF CELL BIOLOGY · VOLUME 86 AUGUST 1980 568-575

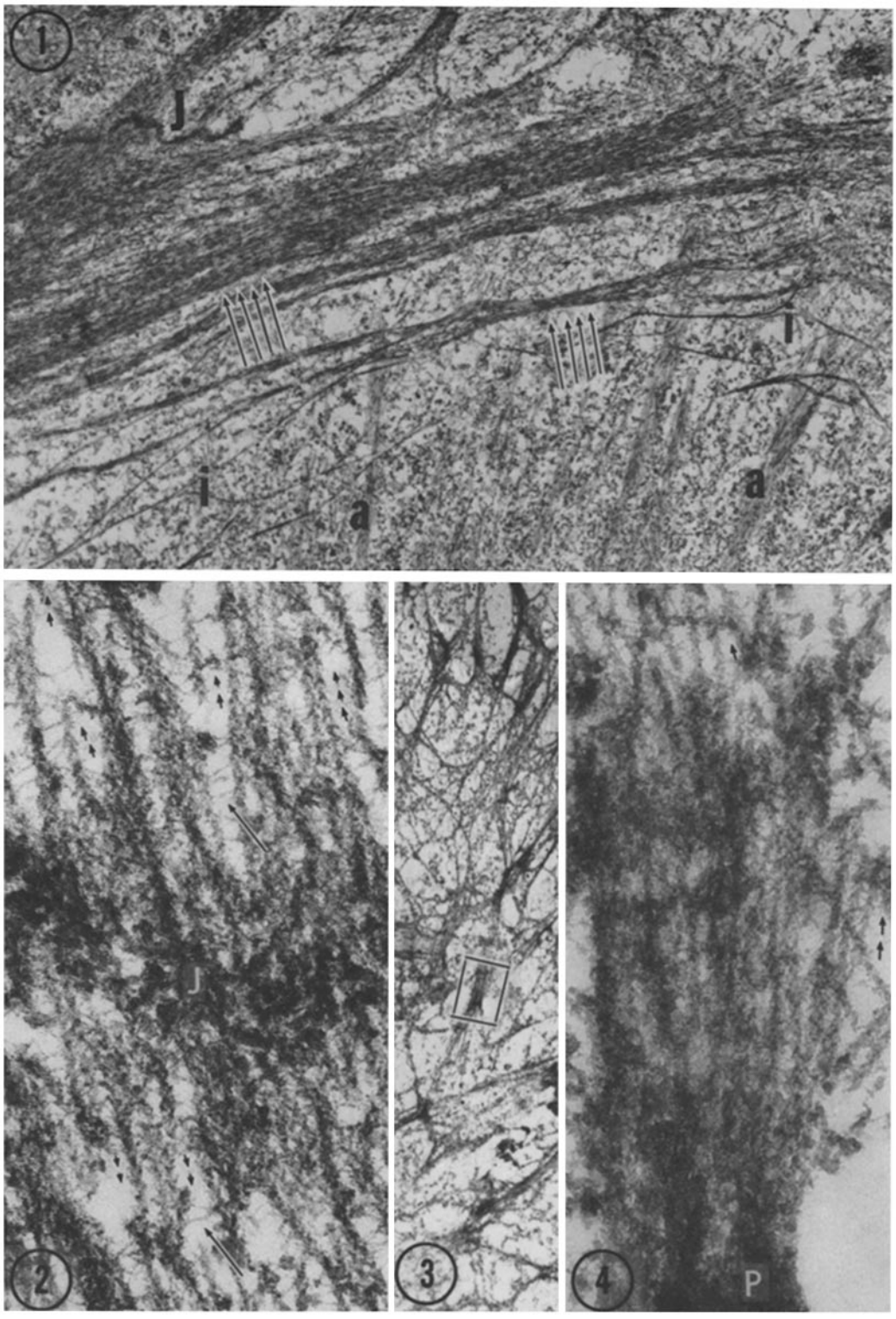

FIGURE 1 Low power view of cells treated with cold ethanol, HMM, and tannic acid. Junctions (*J*), striated stress fibers (arrows), unbanded actin bundles (*a*) and intermediate filaments (*i*) can be seen. × 6,300.

FIGURE 2 Junction (*J*) between two cells with decorated actin filaments (small arrowheads) and short, undecorated fine filaments (arrows) extending laterally from the actin filaments. The decorated actin filaments point away from the junction. × 76,000.

FIGURE 3 Section at interface between substrate and cell. One of the attachment plaques (rectangle) is shown at higher magnification in Fig. 4. × 4,600.

FIGURE 4 The decorated actin filaments (arrowheads) pointing away from the plaque (*P*). × 64,600.

rat kangaroo cells, both in stress fibers and, unexpectedly, in cleavage rings. The polarity of the actin filaments with respect to these striations is described and a model proposed to explain how the stress and cleavage ring fibers are constructed.

MATERIALS AND METHODS

Rat kangaroo cells (PtK_2) were grown as previously described (34). HMM labeling was achieved by removing the medium from the culture dish and adding cold ethanol (−20°C) for 5 min, followed by several rinses during a 5-min period with a low-salt solution (0.1 M KCl, 0.01 M phosphate buffer, 0.001 M $MgCl_2$, pH 7.0). HMM, at concentrations of 0.5–5 mg/ml in low salt, was added to the cells for 1–10 h (35), after which the unbound HMM was removed with several low-salt rinses. Both control and HMM-stained cells were fixed for 30 min in 1% glutaraldehyde buffered in 0.1 M phosphate to which had been added 0.2% tannic acid in 0.1 M phosphate (3). Other control cells were treated with 2% glutaraldehyde in 0.1 M phosphate buffer with no tannic acid added. All cells were then washed several times with the buffer and osmicated for 30 min in 0.5% OsO_4 in phosphate buffer, pH 6.0. After several distilled water rinses, the cells were stained en bloc in 1% aqueous uranyl acetate for 30–45 min. Dehydration was carried out in the culture dishes with ethanol, followed by embedding in Epon. After 3 d in a 60°C oven, the plastic wafer was removed from the culture dish and examined with phase microscopy. Cells were then circled, cut out, and mounted for thin sectioning. Sections were stained with uranyl acetate and lead citrate before viewing in either a JEOL 100 or a Phillips 201 electron microscope.

RESULTS

Rat kangaroo cells (PtK_2), like many other large, flat cells grown in tissue culture, have an extensive array of long stress fibers associated with the cell membrane adjacent to the substratum (Fig. 1). As first shown by Goldman et al. (14) for baby hamster kidney (BHK-21) cells, addition of tannic acid to the usual glutaraldehyde fixation procedure causes the stress fibers to appear banded. In PtK_2 cells fixed with glutaraldehyde alone, periodic densities are seen only infrequently in stress fibers (see also reference 14). When rat kangaroo cells were fixed either directly in glutaraldehyde and tannic acid or pretreated with ethanol at −20°C for 5 min and HMM for 1–10 h and then fixed with glutaraldehyde-tannic acid, many but not all stress fibers appeared banded. The ethanol-HMM treatment did not affect the coherence of the stress fibers or the periodicity of the bands.

On a light and electron microscope level, the stress fibers often appear to run in continuous bundles from one contiguous cell to another. Actually, junctions exist between adjacent PtK_2 cells, and stress fiber bundles insert on either side of these junctions (Figs. 1 and 2). The orientation of HMM arrowheads on the filaments inserting on one side of a junction is always in one direction, pointing away from the membrane (Fig. 2). In adjacent cells, therefore, the filaments in a stress fiber on one side of a junction are opposite in polarity to the filaments on the other side of the junction. Individual decorated filaments can be followed for up to 0.6 μm in a section while bundles of uniformly decorated filaments extend for as long as 1.4 μm from the junctions. In addition to decorated microfilaments, a few short smooth filaments ~10 nm in diameter can be seen running parallel with the microfilaments. Short, fine filaments

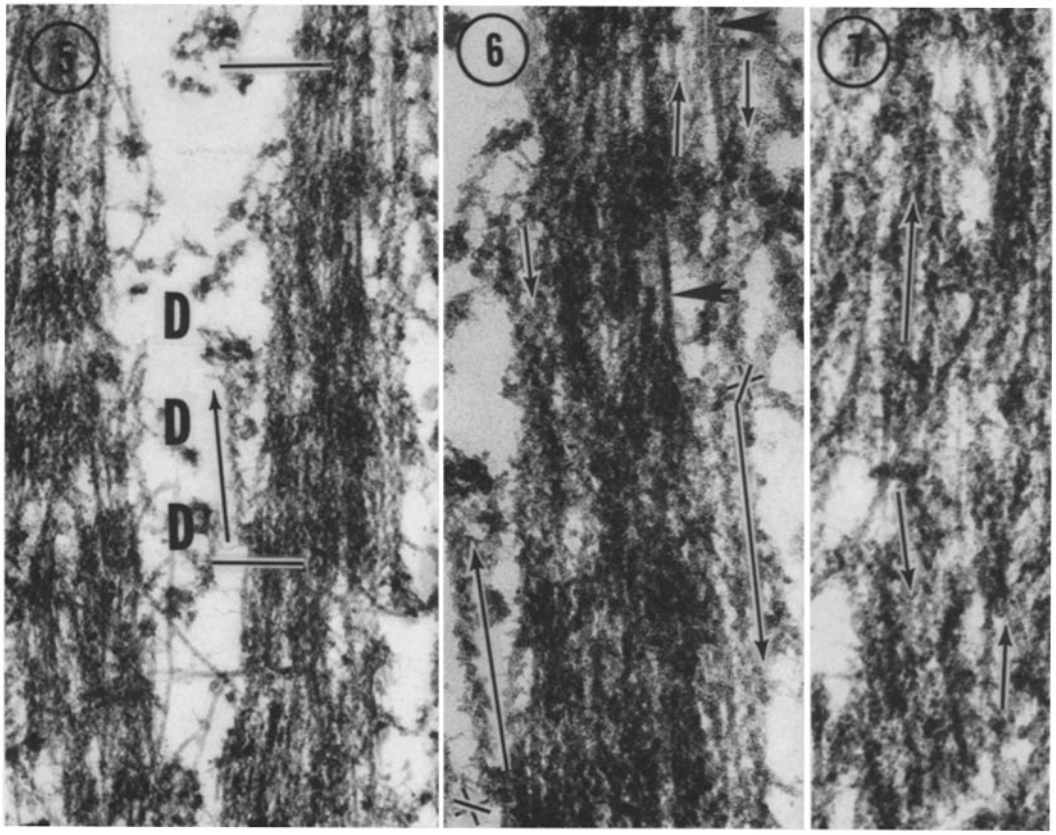

FIGURE 5 Striated stress fiber with individual filament (arrow) extending from one dark band (*D*) past the next. Horizontal lines indicate enlarged area in Fig. 6. × 57,000.

FIGURE 6 Higher magnification of area in Fig. 5. Arrows indicate polarity of actin filaments. Arrowheads point to undecorated thick filaments, one of which (in the upper right corner) is flanked by two oppositely polarized thin filaments. Asterisks are placed beside putative attachment sites of two different actin filaments. × 90,000.

FIGURE 7 Arrows indicate polarity of actin in an unbanded stress fiber. × 95,000.

~4 nm in diameter project laterally from many of the decorated filaments (Fig. 2).

Grazing sections of the cell surface in contact with the substrate show numerous densities or plaques from which microfilaments project (Fig. 3). Amorphous material is usually associated with the microfilaments at this level in the cell, obscuring the arrowhead orientation on many of the filaments (Fig. 4). The discernible arrowheads, though, were always found to point away from the dense plaque. Groups of filaments with the same polarity extended up to 1.9 μm from the plaque.

The stress fibers above the plaque level in the cytoplasm are often banded in appearance (Figs. 1, 5, and 6). Although the margins of the bands are not clearly delineated, approximate measurements of band widths can be made. The distance between the centers of the dark bands averaged 0.32 μm with the dark and light bands each measuring about one-half of that length. HMM-decorated filaments and, less frequently, undecorated filaments 10 nm in diameter are both found in the banded stress fiber (Fig. 6). The undecorated 10-nm filaments, when they can be seen in the banded fibers, seem to be confined to the light bands. Bundles of 10-nm filaments are also seen adjacent to stress fibers, often intersecting the fibers (not shown).

Individual actin filaments are seen most clearly at the periphery of the banded fibers where they appear to be as long as 0.6 μm. The filaments pass through both light and dark bands of the stress fiber and different filaments within the same band can be opposite in polarity (Figs. 5 and 6). In a few cases where an actin filament appeared to originate at a dense band, the arrowheads pointed away from the putative attachment point (Fig. 6). In addition to banded fibers, unbanded stress fibers were also found in all the cells surveyed (Fig. 1). They sometimes have oppositely polarized actin filaments (Fig. 7), and in other cases filaments are oriented primarily in one direction. Within these unbanded stress fibers, areas of similarly oriented filaments extended for 1.8 μm while individual decorated filaments can be followed in a section for distances up to 0.6 μm. In the unbanded stress fibers, undecorated filaments, 10 nm in diameter, can also be seen among the actin filaments.

Sections through cleaving cells opened in cold ethanol, stained with HMM, and fixed with tannic acid, show that actin filaments are aligned in the cleavage furrow in the same banded pattern as seen in stress fibers (Figs. 8 and 9). These banded bundles were found only in the cleaving region of the cell because stress fibers are not present in the cytoplasm during this part of the cell cycle. In cleaving cells the distance between dark bands is similar to that in stress fibers, varying from 0.26 to 0.35 μm with the light and dark bands usually each measuring one-half of that value. Undecorated as well as decorated filaments are present in the contractile ring. The undecorated filaments are ~10 nm in diameter and at least 0.15 μm long. They are seen more easily in the light bands, but it appears that they may penetrate into the dark bands in some cases. Arrowheads can be seen in both the light and dark bands. Individual HMM-decorated filaments at the periphery of a bundle measure as long as 0.6 μm, and within a bundle the neighboring filaments sometimes have opposite polarities and in other cases the same orientation.

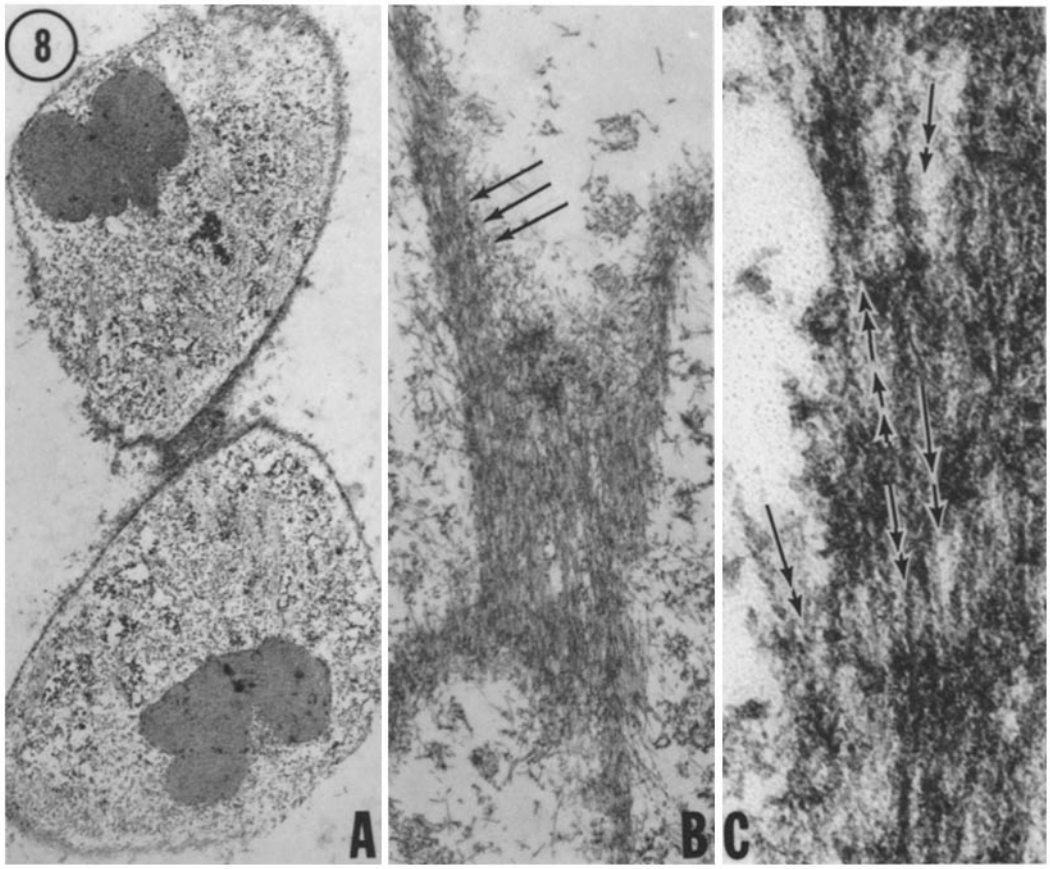

FIGURE 8 (*A*) Cleaving cell at low magnification. (*B*) Higher magnification showing light and dark bands (arrows). (*C*) Arrows indicate polarity of actin filaments in dark and light bands. (*A*) × 3,000; (*B*) × 14,000; (*C*) × 95,000.

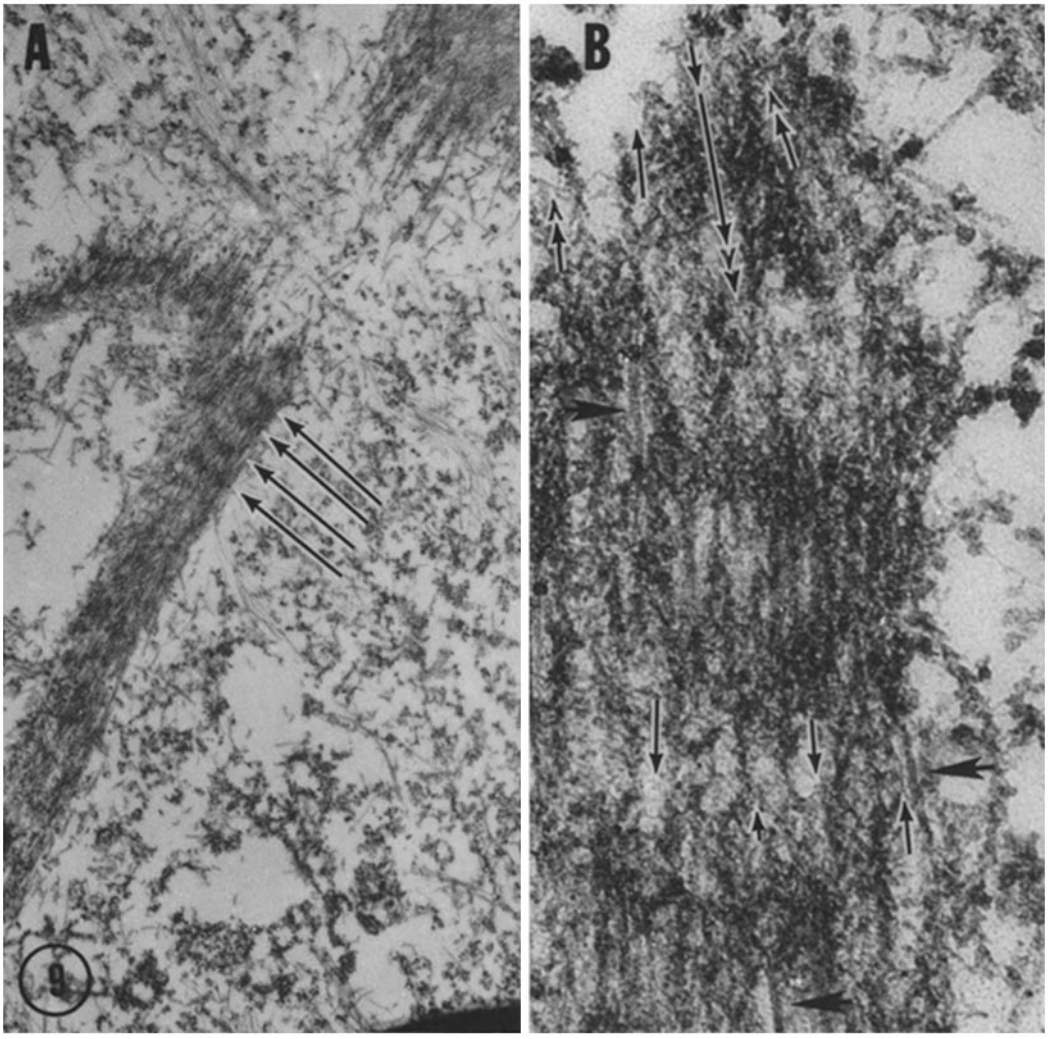

FIGURE 9 (*A*) Portion of cleavage furrow from different cell showing banded (arrows) pattern. (*B*) Vertical arrows indicate polarity of actin filaments and horizontal arrows indicate undecorated thick filaments. (*A*) × 14,000; (*B*) × 95,000.

Other cleaving cells in which a mid-body is present (Fig. 10) show no banding of actin filaments. As in the banded cleavage furrows, adjacent actin filaments are sometimes identical in polarity and sometimes antiparallel. The actin filaments are more loosely associated in these late cleavage cells, and fine fibrils often extend laterally from them, reminiscent of the fine fibrils associated with the actin filaments of a cell junction (Fig. 2). Individual actin filaments can be followed in these areas for ~0.6 μm. Undecorated 10-nm filaments were seen less frequently among these actin filaments than is the case when the cleavage furrow is in a banded pattern.

DISCUSSION

The usual procedure for making nonmuscle cells permeable to HMM has been glycerination (7, 9, 20, 34, 36), a technique first devised for muscle (48). We have substituted −20°C ethanol for glycerol after finding that no actin was released from cells plunged into cold ethanol for 5 min, whereas significant amounts were extracted with glycerol (41). Although beautiful arrowheads were obtained by Begg et al. (3) using glycerol, we found that substitution of ethanol, followed by HMM staining and tannic acid fixation (3, 44), gave improved ultrastructural preservation. (Compare Fig. 1 with reference 3, Fig. 4*b*).

The extensive arrays of oriented cytoplasmic fibers found in many nonmuscle cells have been considered cytoskeletal elements (4, 52) as well as contractile (4). It is known from micromanipulation studies that cells with stress fibers develop tension (6, 4). The force developed in a sheet of fibroblasts was measured by James and Taylor (21) and calculated to be about $\frac{1}{100}$th the tension developed by frog skeletal muscle and $\frac{1}{20}$th that developed by bovine smooth muscle. More recently, Isenberg et al. (19) used a laser to surgically isolate a stress fiber and then induce shortening with ATP. These observations coupled with the discovery that actin, myosin, tropomyosin, and α-actinin are localized in cytoplasmic stress fibers (21–25, 31, 34, 51, 54) suggest that stress fibers may be similar in construction to muscle fibers (22, 31, 33, 51).

During cytokinesis there is no doubt that contractile force is developed in the cleavage furrow, and Schroeder (42, 43) proposed in 1968 that a sliding filament mechanism analogous to muscle contraction provided the force. Our finding that actin filaments are organized in similar arrays in both stress fibers and cleavage furrows leads us to suggest that both exert force by similar mechanisms. We have found that oppositely polarized actin filaments are present not only in stress fibers as has been noted by Begg et al. (3), but also in the cleavage ring, and that the filaments within the fibers of both systems are oriented in the same banded pattern (Figs. 1, 5, 8, and 9). The

major constituents of both dark and light bands are decorated actin filaments. Within the fiber the filaments are usually packed too densely to make it possible to determine filament length or orientation. However, in favorable sections, arrowheads can be seen within fibers (Figs. 6, 8 *C*, 9 and *B*), and filament length can be followed both at sites where actin inserts on the membrane as in cell junctions (Fig. 2), and sometimes at the edges of the banded fibers (Fig. 6) where they extend for several band widths with arrowhead orientation pointing away from putative attachment points (Fig. 6).

Others have seen similar striations in stress fibers on an ultrastructural level with and without tannic acid (13–15, 33), and with fluorescent antibody staining against myosin, (11, 51), tropomyosin (22, 23) and α-actinin (15, 23, 24), and actin (25). The dimensions of the dark bands and light bands differ markedly in the five ultrastructural studies, as can be seen in Table I. The bands described in this paper for PtK_2 are extremely small when compared with the bands in fibroma cells (15) and BHK cells (14), but are comparable to the band sizes in aortic endothelial cells (13). Different band sizes may be caused by differences in fixation, or may reflect the degree of contraction of the fiber. They may also be caused by cell type, reflecting a variation comparable to that found in sarcomeres of different types of muscles (38). The fact that the bands were the same in control cells which were not exposed to ethanol as they were in ethanol-treated cells indicates that ethanol is not a factor.

By analogy with muscle cells, the actin filaments of the stress fibers should be polarized so that HMM decoration produces arrowheads which all point away from the membrane and toward the direction of force. This is precisely the case at the junctions between two cells (Fig. 2) and at the electron-dense plaques (Fig. 4) found in the first one or two *en face* sections (Fig. 3), presumably corresponding to the plaques described by Abercrombie et al. (1) and Singer (45), as forming points of adherence of a cell to the substrate. Cytoplasmic actin filaments have also been shown to be oriented with arrowheads pointing away from membrane association sites in microvilli (3, 5, 20, 27), acrosomal filaments of sperm (50), platelet microspikes (28), coelomocytes (8), and beneath the plasma membrane of tissue culture cells (3, 46).

Not all of the stress fibers examined in this study were banded (Figs. 1 and 7), nor were the microfilaments in a banded arrangement in the furrow of cells in which cleavage had advanced to the mid-body stage (Fig. 10). In both unbanded stress fibers and furrows of mid-body stage cleaving cells, the actin filaments were approximately parallel to one another with the orientation of adjacent filaments sometimes identical and in other cases opposite in polarity. In the cleavage ring, which is a transient structure, the unbanded arrangement of the actin filaments probably results from the disassembly of the ring. Whether unbanded stress fibers are in a state of transition to or from a banded form, is not possible to determine.

Undecorated filaments ~10 nm in diameter are found adjacent to the actin filaments in the light bands (Figs. 6 and 9 *B*). Their ends seem to be embedded in the dark bands, making them at least as long as a light band, 0.15 μm, and conceivably

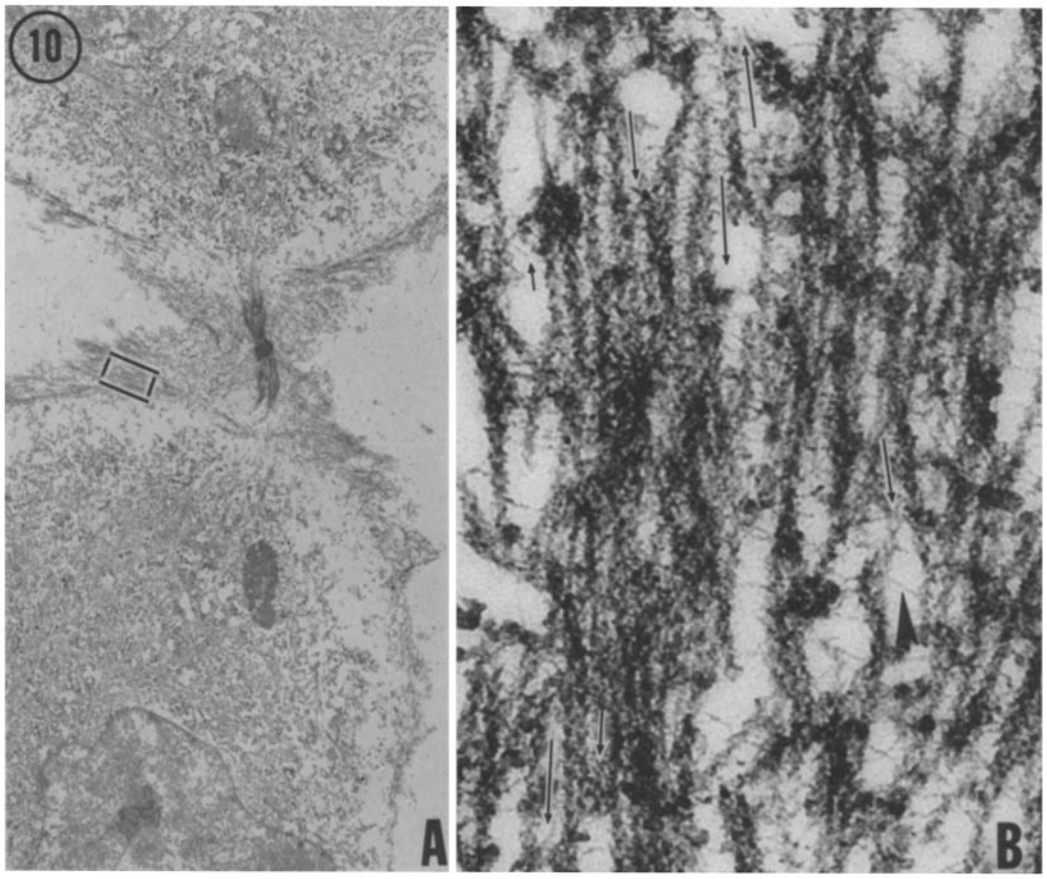

FIGURE 10 (*A*) Cleaving cell with mid-body. Area in box is shown enlarged in *B*. (*B*) Arrows indicate actin filament polarity. Note series of fine filaments (arrowhead) extending from microfilaments. These are similar to ones observed near cell junctions. (*A*) × 4,600; (*B*) × 76,000.

as long as the distance between the centers of two dark bands, 0.26–0.35 μm. Synthetic nonmuscle myosin filaments (26, 29, 53) are ~10 nm in diameter and ~0.3–0.5 μm long and, thus, are similar to the filaments we observe. The PtK_2 cells, however, have large numbers of 10-nm intermediate filaments (10, 36) which sometimes run parallel to the stress fibers (Fig. 1). In cleavage furrows, intermediate filaments run through the middle of the cleavage ring (Fig. 9) and also along the edges of the furrow. We do not think that the undecorated filaments seen within the light bands of the fibers are intermediate filaments because they are very short as opposed to the long intermediate filaments, and because at high magnification they lack the beaded substructure seen in the intermediate filaments.

Anti-a-actinin staining of a variety of tissue culture cells results in fluorescent bands which are 0.2–0.5 μm separated by nonstaining region of 1–1.5 μm (15, 23, 31, 54). The 0.15-μm width for the dark bands in PtK_2 cells would be expected to give rise to fluorescent anti-*a*-actinin bands of the reported range, 0.2–0.5 μm, separated by nonstaining bands of equal width. (Preliminary staining results with α-actinin antibody carried out in collaboration with Dr. Brigitte Jockusch (European Molecular Biology Laboratory, Heidelberg, W. Germany) show this to be true). Gordon (15) has compared ultrastructural band widths with fluorescent anti-α-actinin band widths in one cell type and has concluded that α-actinin is localized in the dark ultrastructural band. In striated muscle cells, α-actinin is localized in the Z bands (20), the sites of actin filament attachments. Our observation that actin filaments sometimes originate at the level of the dark band is compatible with the idea that α-actinin is present in this band.

TABLE I

Stress Fiber Striations Observed in the TEM

Cell type	Dark band	Light band	Reference
	μm		
Fibroma	0.4	0.7	15
BHK-21	0.3	0.28	14
Rat endothelial	0.1	0.46	33
Rat hypertensive endothelial	0.18	0.18	13
PtK_2	0.16	0.16	This paper

Model

Contraction of a sarcomere of cross-striated muscle occurs when two groups of oppositely polarized actin filaments are pulled in by myosin filaments (Fig. 11 *a*). The actin filaments can then overlap and slide past one another until they or the myosin-thick filaments collide with the Z disks (17). In vertebrate striated muscles, the thick filament (1.6 μm) is longer than the thin filament (1.0 μm) (17, 18) and thus, during contraction, would meet the Z line first. In muscles where the actin attachment site is not a solid Z disk but porous or composed of dense bodies, contraction can cause myosin and actin filaments to slide past one another and past the dense bodies as well (2, 16, 37).

In contrast to cross-striated muscles, actin filaments in nonmuscle cells appear to be much longer than myosin filaments (26, 27). Synthetic and putative natural nonmuscle myosin filaments from vertebrates appear to be ~0.25–0.3 μm in length (26, 27, 29). Our measurements of actin filaments in PtK_2 cells indicate that they are at least 0.6 μm, and possibly as long as 1.9 μm. In a sliding filament model of contraction (Fig. 11 *b*), the thin filaments would reach the opposite actin attachment site long before the thick filaments.

Our results support a sarcomeric model as drawn in Fig. 11 *c*. To simplify, we have taken the length of the thin filament to be a uniform 0.6 μM length, although it may be greater and may be variable (32). Individual thin filaments are shown anchored in a dense band which we predict contains α-actinin

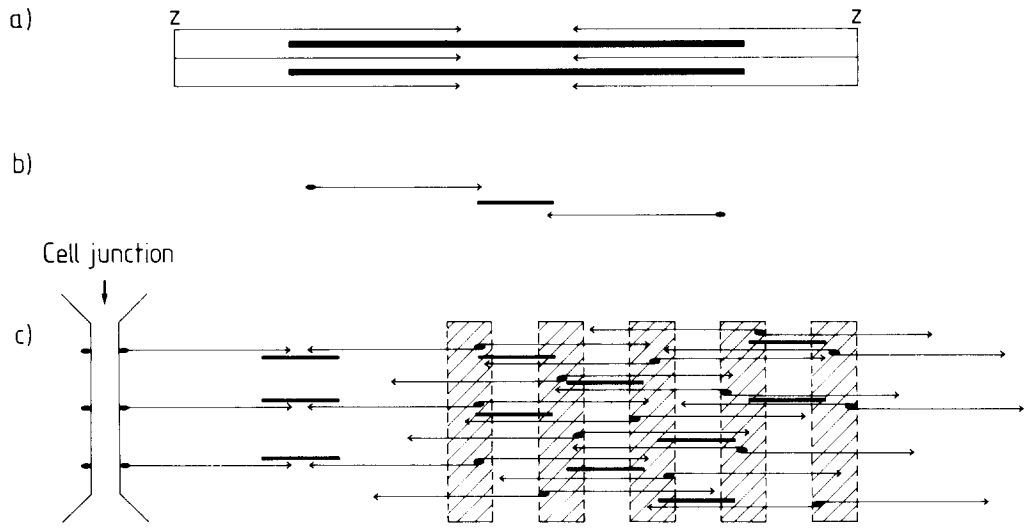

FIGURE 11 All three parts of this diagram are drawn so that the thin filaments have the same diameter while the thick filaments in muscle (*a*) have a larger diameter (18 nm) than the thick filaments in the nonmuscle sarcomeric model (*b* and *c*) (10 nm). The length of the thin filaments extending from the Z line (*a*) are 1.0 μm while the lengths of the thin filaments extending from the middle of the dense bodies (*b* and *c*) are 0.6 μm. The arrowheads indicate the polarity and ends of the actin filaments. Only two actin filaments are shown attached to each dense body, and the dense bodies are separated from each other for clarity. On contraction, the thick filaments in the muscle sarcomere (*a*) would approach the Z line before the thin filaments because of their greater lengths. In contrast, the contraction of the nonmuscle model would result in the thin filaments approaching the actin attachment sites before the thick filaments. In the highly contracted part of the stress fiber, these thin filaments almost extend past two consecutive sets of actin attachment sites (dark bands, *c*) before the short myosin filaments passed the first actin attachment sites. Further details of the model are discussed in the text.

material similar to that found in Z bands (46, 47). Not only is there a double overlap of thin filaments in the light band as opposite sets of actin filaments slide past one another, but additional overlap occurs when the filaments pass through into the next sarcomeric unit. This would explain why adjacent actin filaments in both dark and light bands are sometimes opposite in polarity and in other cases have the same polarity.

In our model the myosin is in the light bands (Fig. 11 *c*). Anti-myosin staining would, in this case, give a banded pattern as has been observed in other cells (11, 14, 51, 53, 54). Greater contraction, causing the myosin to penetrate through the dense band, would produce continuous staining. This type of staining can be seen in published papers but is not discussed (14, 51). Depending on the degree of contraction, double staining with anti-myosin and α-actinin would yield either a continuous pattern as observed by Gordon (15) or a discontinuous pattern as reported by Zigmond et al. (54). The model is also compatible with the continuous staining usually observed with fluorescent HMM or actin antibody (25, 35). The rare periodic pattern of actin localization (15, 35) would result from a stretched version of our model (Fig. 11 *b*). It is difficult to interpret the periodic tropomyosin localization patterns (22, 23) in terms of this model unless we assume, as Lazarides suggests (22), that some substance (we suggest α-actinin) associated with the actin in a regular spacing prevents tropomyosin antibody binding but not actin antibody binding.

There may, of course, be no simple correlation between fluorescent antibody staining patterns and dark and light bands seen ultrastructurally. The interdigitation or interactions of filaments with each other or with α-actinin may make regions along the fibers inaccessible to antibody staining. Work by Pepe (30) on muscle beautifully illustrates the different antibody staining patterns which can be obtained when myosin antibodies are used to stain sarcomeres in varying states of contraction. Many more studies on nonmuscle cells, coupling antibody staining with ultrastructural studies, are needed before the sarcomere-like structures in nonmuscle cells can be defined in as much detail as sarcomeres in muscle cells.

This work was supported by grants from the National Institutes of Health (HL-15835 to the Pennsylvania Muscle Institute and GM 22293 and GM 25653 to J. W. Sanger).

Received for publication 23 August 1979, and in revised form 21 April 1980.

REFERENCES

1. Abercrombie, M. J., E. M. Heaysman, and S. M. Pegrum. 1971. The locomotion of fibroblasts in culture. IV. Electron microscopy of the leading lamella. *Exp. Cell Res.* 67: 359–367.
2. Aronson, J. 1963. Overlap of the birefringement component of adjacent A regions during the induced shortening of fibrils leased from *Drosophila* muscle. *J. Cell Biol.* 19:107–114.
3. Begg, D. A., R. Rodewald, and L. I. Rebhun. 1978. Visualization of actin filament polarity in thin sections. *J. Cell Biol.* 79:846–852.
4. Buckley, J. K., and K. R. Porter. 1967. Cytoplasmic fibrils in living cultured cells. *Protoplasma.* 64:349–380.
5. Burgess, D. R., and T. E. Schroeder. 1977. Polarized bundles of actin filaments within microvilli of fertilized sea urchin eggs. *J. Cell Biol.* 74:1032–1037.
6. Chambers, R., and H. B. Fell. 1931. Micro-operations in cells in tissue culture. *Proc. Roy. Soc. London Ser. B.* 109:380–403.
7. Chang, C. M., and R. D. Goldman. 1973. The localization of actin-like fibers in cultured neuroblastoma cells as revealed by heavy meromyosin binding. *J. Cell Biol.* 57:867–874.
8. Edds, K. T. 1977. Microfilament bundles I. Formation with uniform polarity. *Exp. Cell Res.* 108:452–456.
9. Forer, A., and O. Behnke. 1972. An actin-like component in spermatocytes of a crane fly (*Nephrotoma* suturalis Loew). 1. The spindle. *Chromosoma (Berl.).* 39:145–173.
10. Franke, W. W., C. Grund, M. Osborn, and K. Weber. 1978. The intermediate-sized filaments in rat kangaroo PtK_2 cells. I. Morphology in situ. *Cytobiologie* 17:365–391.
11. Fujiwara, K., and T. D. Pollard. 1976. Fluorescent antibody localization of myosin in the cytoplasm, cleavage furrow, and mitotic spindle of human cells. *J. Cell Biol.* 71:848–875.
12. Fujiwara, K., M. E. Porter, and T. D. Pollard. 1978. Alpha-actinin localization in the cleavage furrow during cytokinesis. *J. Cell Biol.* 79:268–275.
13. Gabbiani, G., G. Elemer, Ch. Guelpa, M. B. Vallotton, M.-C. Badonnel and I. Hüttner. 1979. Morphologic and functional changes of the aortic intima during experimental hypertension. *Am. J. Pathol.* 96:399–422.
14. Goldman, R. D., B. Chojnacki, and M. J. Yerna. 1979. Ultrastructure of microfilament bundles in baby hamster kidney (BHK-21) cells. *J. Cell Biol.* 80:759–766.
15. Gordon, W. E. 1978. Immunofluorescent and ultrastructural studies of sarcomeric units in stress fibers of cultured nonmuscle cells. *Exp. Cell Res.* 117:253–260.
16. Hoyle, G., J. H. McAlear, and A. Selverston. 1965. Mechanism of supercontraction in a striated muscle. *J. Cell Biol.* 26:621–640.
17. Huxley, H. E. 1961. The contractile structure of cardiac and skeletal muscle. *Circulation.* 24:328–335.
18. Huxley, H. E. 1963. Electron microscope studies on the structure of natural and synthetic protein filaments from striated muscles. *J. Mol. Biol.* 7:281–308.
19. Isenberg, G., P. C. Rathke, N. Hülsmann, W. W. Franke, and K. E. Wohlfarth-Bottermann. 1976. Cytoplasmic actomyosin fibrils in tissue culture cells. *Cell Tissue Res.* 166: 427–443.
20. Ishikawa, H., R. Bischoff, and H. Holtzer. 1969. Formation of arrowhead complexes with heavy meromyosin in a variety of cell types. *J. Cell Biol.* 43:312–328.
21. James, D. W., and J. F. Taylor. 1968. The stress developed by sheets of chick fibroblasts *in vitro*. *Exp. Cell Res.* 54:107–110.
22. Lazarides, E. 1975. Tropomyosin antibody: The specific localization of tropomyosin in non-muscle cells. *J. Cell Biol.* 65:549–561.
23. Lazarides, E. 1976. Actin, alpha-actinin and tropomyosin interaction in the structural organization of actin filaments in non-muscle cells. *J. Cell Biol.* 68:202–219.
24. Lazarides, E., and K. Burridge. 1975. Alpha-actinin: Immunofluorescent localization of a muscle structure protein in nonmuscle cells. *Cell.* 6:289–298.
25. Lazarides, E., and K. Weber. 1974. Actin antibody: The specific visualization of actin filaments in non-muscle cells. *Proc. Natl. Acad. Sci. U. S. A.* 71:2268–2272.
26. Mooseker, M. S., T. D. Pollard, and K. Fujiwara. 1978. Characterization and localization of myosin in the brush border of intestinal epithelial cells. *J. Cell Biol.* 79:444–453.
27. Mooseker, M. S., and L. G. Tilney. 1975. Organization of an actin filament-membrane complex. *J. Cell Biol.* 67:725–743.
28. Nachmias, V. T., and A. Asch. 1976. Regulation and polarity: Results with myxomycete and with human platelets. *Cold Spring Harbor Conf. Cell Proliferation.* 3:771–783.
29. Niederman, R., and T. D. Pollard. 1975. *In vitro* assembly and structure of myosin filaments. *J. Cell Biol.* 67:72–92.
30. Pepe, F. A. 1975. Structure of muscle filaments from immunohistochemical and ultrastructureal studies. *J. Histochem. Cytochem.* 23:543–562.
31. Rathke, P. C., M. Osborn, and K. Weber. 1979. Immunological and ultrastructural characterization of microfilament bundles: polygonal nets and stress fibers in an established cell line. *Eur. J. Cell. Biol.* 19:40–48.
32. Robinson, T. F., and S. Winegrad. 1979. The measurement and dynamic implication of thin filament lengths in heart muscle. *J. Physiol. (Lond.).* 286:607–619.
33. Röhlick, P., and I. Olah. 1967. Cross-striated fibrils in the endothelium of the rat myometral arterioles. *J. Ultrastruct. Res.* 18:667–676.
34. Sanger, J. W. 1975. The presence of actin during chromosomal movement. *Proc. Natl. Acad. Sci. U. S. A.* 72:2451–2455.
35. Sanger, J. W. 1975. Intracellular localization of actin with fluorescently labelled heavy meromyosin. *Cell Tissue Res.* 161:431–444.
36. Sanger, J. W. 1977. Nontubulin molecules in the spindle. Mitosis: Facts and Questions. M. Little, N. Paweletz, C. Petzelt, H. Ponstingle, D. Schroeter, and H.-P. Zimmermann, editors. Springer-Verlag, New York. 98–113.
37. Sanger, J. W., and R. B. Hill. 1973. The contractile apparatus of the radular protractor muscle of *Busycon canaliculatum*. *Proc. Malacol. Soc. Lond.* 40:335–341.
38. Sanger, J. W., and F. V. McCann. 1968. Ultrastructure of moth alary muscles and their attachment to the heart wall. *J. Insect Physiol.* 14:1539–1544.
39. Sanger, J. W., and J. M. Sanger. 1976. Actin localization during cell division. *Cold Spring Harbor Conf. Cell Proliferation.* 3:1295–1316.
40. Sanger, J. W., and J. M. Sanger. 1979. The cytoskeleton and cell division. *Meth. Achiev. Exp. Pathol.* 8:110–142.
41. Sanger, J. W., J. M. Sanger, and J. Gwinn. 1979. Actin and the mitotic spindle in cell function. F. A. Pepe, J. W. Sanger, and V. Nachmias, editors. Academic Press, Inc., New York. 313–323.
42. Schroeder, T. E. 1968. Cytokinesis: Filaments in the cleavage furrow. *Exp. Cell Res.* 53: 272–276.
43. Schroeder, T. E. 1975. Molecules and cell movement. S. Inoué and R. E. Stephens, editors. Raven Press, New York. 305–332.
44. Seagull, R. W., and I. B. Heath. 1979. The effects of tammic acid on the *in vivo* preservation of microfilaments. *Eur. J. Cell Biol.* 20:184–188.
45. Singer, I. I. 1979. The fibronexus: a transmembrane association of fibronectin-containing fibers and bundles of 5 nm microfilaments in hamster and human fibroblasts. *Cell.* 16: 675–685.
46. Small, J. V., G. Isenberg, and J. E. Celis. 1978. Polarity of actin at the leading edge of cultured cells. *Nature (Lond.).* 272:638–639.
47. Stromer, M. H., and D. E. Goll. 1972. Studies on purified α-actinin and tropomyosin to Z-line extracted myofibrils. *J. Mol. Biol.* 67:489–494.
48. Szent-Gyorgyi, A. 1951. Chemistry of Muscular Contraction. Academic Press, Inc., 2nd edition.
49. Szent-Gyorgyi, A. G., C. Cohen, and J. Kendrick-Jones. 1971. Paramyosin and the filaments of molluscan "catch" muscles. II. Native filaments: Isolation and characterization. *J. Mol. Biol.* 56:239–258.
50. Tilney, L. G., and N. Kallenbach. 1979. Polymerization of actin. VI. The polarity of the actin filaments in the acrosomal process and how it might be determined. *J. Cell Biol.* 81: 608–623.
51. Weber, K. and V. Groeschel-Stewart. 1974. Antibody to myosin: The specific visualization of myosin containing filaments in non-muscle cells. *Proc. Natl. Acad. Sci. U. S. A.* 71: 4561–4563.
52. Wilson, E. B. 1928. The Cell in Development and Heredity, 3rd Edition. Macmillan, Inc., New York.
53. Yerna, M. J., M. O. Aksoy, D. J. Hartshorne, and R. D. Goldman. 1978. BHK 21 Myosin: Isolation, biochemical characterization and intracellular localization. *J. Cell Sci.* 31:411–429.
54. Zigmond, S. H., J. J. Otto, and J. Bryan. 1979. Organization of myosin in a submembranous sheath in well-spread human fibroblasts. *Exp. Cell Res.* 119:205–219.